

1 DIRECT MEASUREMENTS OF CO₂ FLUX IN THE GREENLAND SEA

2
3 Siv K. Lauvset^{1,2}; Wade R. McGillis^{3,4}; Ludovic Bariteau⁵; C.W. Fairall⁶; Truls
4 Johannessen^{1,2,7}; Are Olsen^{7,2}; Christopher J. Zappa^{3,4}

5
6 ¹Geophysical Institute, University of Bergen, Norway, siv.lauvset@gfi.uib.no

7 ²Bjerknes Centre for Climate Research, Bergen, Norway

8 ³Department of Earth and Environmental Engineering, Columbia University, New York, NY,
9 USA

10 ⁴Lamont Doherty Earth Observatory, Columbia University, Palisades, NY, USA

11 ⁵Cooperative Institute for Research in Environmental Sciences (CIRES), University of
12 Colorado, Boulder, Colorado, USA

13 ⁶NOAA Earth System Research Laboratory, Boulder, CO, USA

14 ⁷Uni Bjerknes Centre, Bergen, Norway

15 16 ABSTRACT

17 In summer 2006 eddy correlation CO₂ fluxes were measured in the Greenland Sea. A
18 novel system set-up with two shrouded LICOR-7500 detectors was used. One detector was
19 used exclusively to determine, and allow the removal of, the bias on CO₂ fluxes due to sensor
20 motion. A recently published correction method for the CO₂-H₂O cross-correlation [*Prytherch*
21 *et al.*, 2010a] was applied to the data set. We show that even with shrouded sensors the data
22 require significant correction due to this cross-correlation. This correction adjusts the average
23 CO₂ flux by an order of magnitude from $-6.7 \times 10^{-2} \text{ mol m}^{-2} \text{ day}^{-1}$ to $-0.61 \times 10^{-2} \text{ mol m}^{-2} \text{ day}^{-1}$,
24 making the corrected fluxes comparable to those calculated using the *Wanninkhof* [1992]
25 parameterization for transfer velocity.

26 INTRODUCTION

27 Because the atmospheric CO₂ concentration is rising due to the burning of fossil fuels,
28 land use change, and cement production it is important to accurately quantify the size of the
29 total ocean carbon sink and its variations with time. For this we need to know the air-sea CO₂
30 flux. Because it is difficult to measure the global air-sea CO₂ flux, estimates rely mostly on
31 calculations on the form

$$32 F_{\text{CO}_2} = k S \Delta f_{\text{CO}_2} \quad (1)$$

33 where $\Delta f\text{CO}_2$ is the difference between the fugacity of CO_2 ($f\text{CO}_2$) in the sea and in the air, S
34 is the gas solubility, and k is an estimate of the gas transfer velocity usually parameterized as
35 a function of wind speed (U_{10N}). The most widely used parameterizations of k have been
36 derived using tracer release experiments [*Ho et al.*, 2006; *Liss and Merlivat*, 1986;
37 *Nightingale et al.*, 2000], wind-wave tank experiments [*Liss and Merlivat*, 1986], and
38 radiocarbon invasion [*Naegler et al.*, 2006; *Sweeney et al.*, 2007; *Wanninkhof*, 1992]. Yet,
39 none of these capture the complete range of processes relevant to air-sea gas exchange, nor
40 are they consistent at high wind speeds. To resolve these issues we need direct measurements
41 of the air-sea CO_2 flux (F_{CO_2}).

42 Direct measurements of the F_{CO_2} can be carried out using the eddy correlation (EC)
43 method [*McGillis et al.*, 2001a; *McGillis et al.*, 2004; *Wanninkhof and McGillis*, 1999], but
44 after a decade of significant technical advances several difficulties with the EC method still
45 remain. First among these is that the observed EC F_{CO_2} tend to be considerably larger than
46 bulk parameterization or tracer derived fluxes [*Broecker et al.*, 1986; *Kondo and Tsukamoto*,
47 2007; *Prytherch et al.*, 2010a], which have led to few data sets of F_{CO_2} from EC experiments
48 being published. Recent research suggest that the measurements are too high due to a cross-
49 correlation between CO_2 and H_2O stemming from contamination of the exposed sensor
50 optical surfaces by hygroscopic particles [*Prytherch et al.*, 2010a].

51 In this paper we will present the first data set of EC F_{CO_2} measured in the Greenland
52 Sea featuring unique environmental conditions and using a novel instrument set-up. We have
53 used this data set to test whether the PKT correction method [*Prytherch et al.*, 2010a] is
54 suitable for data sets measured in such environmental conditions and with this instrument set-
55 up.

56 EXPERIMENT AND METHODS

57 The data were obtained on the Greenland Sea cruise 58GS20060721 [*Olsen and*
58 *Omar, 2007*], carried out onboard the research vessel *G.O. Sars* between July 21 and August
59 3, 2006. The cruise started in Akureyri, Iceland and ended in Tromsø, Norway. The flux
60 measurement system was set up on a mast located directly above the bow of the ship ~14.5 m
61 above the sea surface. Two open path LICOR-7500 non-dispersive infrared (NDIR) detectors,
62 a 3D Gill Sonic anemometer, a Motionpak, and a compass were collocated on top of the ship
63 mast. The NDIR detectors were mounted ~1 m from the sonic anemometer and motion
64 system, and both were shrouded in rigid plastic housing. The shrouds prevent loss of data due
65 to severe weather conditions and icing, leading to a more robust data set. The instrument set-
66 up is schematically shown in Fig. 1. Air entered the first sensor, hereafter referred to as
67 ‘sample’, at 570 l min^{-1} and passed through a mixing chamber connected to a high volume
68 pump; the intake of the second sensor, hereafter referred to as ‘null’, is taken from the mixing
69 chamber using a second (low volume) flow path at 200 ml min^{-1} . The sensors were mounted
70 next to each other with the long axes aligned vertically so that they experienced the same
71 motion, and the rigid fit in the shroud prevented flexing of the support structures of the
72 detectors. We calculate that the null sensor measurement fluctuations are reduced by 97 %
73 using this set up [*Bariteau et al., 2010*] such that the remaining signal is due to the motion
74 artifact only. Motion contamination was first described by *Fairall et al.* [2000] and correction
75 methods based on covariance with a calibration gas [*McGillis et al., 2001*], a second identical
76 null sensor with a sealed input [*McGillis et al., 2004*], or correlation with measured ship
77 motion variables [*Yelland et al., 2009; Miller et al., 2010*] have been used previously. The
78 LICOR-7500 has much less motion contamination than their closed-path systems, however
79 [*Miller et al. 2009*]. We assume that the motion artifact is the same for both sensors and
80 subtract this from the sample signal on a point-by-point basis.

81 The ship was equipped with an underway pCO₂ system [*Pierrot et al.*, 2009] used to
82 measure the fCO₂ in both the surface ocean and the atmosphere, the sea surface temperature
83 (SST) and the sea surface salinity (SSS). This system is calibrated every 3-4 hours using three
84 referenced standard gases obtained from the National Oceanographic and Atmospheric
85 Administration Climate Monitoring and Diagnostics Laboratory (NOAA/CMDL). Other
86 meteorological variables, such as air temperature, air pressure, and relative humidity, as well
87 as navigation data were retrieved from the ship's measurement system.

88 Collected data were processed in ten-minute blocks and fluxes were obtained by
89 correlating the motion-corrected vertical velocity with the fast fluctuations of interest. For
90 details concerning how the high frequency wind speed measurements were corrected for the
91 ship's movement see *Edson et al.* [1998] and *Miller et al.* [2008]. Only data with suitable
92 wind vectors and with reasonable limits on ship maneuvers and ship motion correction were
93 selected. The flow tilt calculated from the sonic anemometer was also used to account for
94 flow distortion effects [*Fairall et al.*, 1997]. Because of problems with the infrared sensors
95 and the ship compass during the first half of the cruise, the results of this study are mostly
96 based on the last half of the cruise, east of ~7°W. Out of the total 1896 10 minute averages
97 652 passed all quality controls.

98 Both latent heat and CO₂ fluxes were computed from the sample NDIR sensor, while
99 the sensible heat flux was computed from vertical velocity–sonic temperature covariance. The
100 humidity contribution to sonic temperature was removed using the bulk latent heat flux. The
101 effects of humidity and temperature on the CO₂ measurements were removed prior to
102 calculating the flux by converting the measured molar densities into mixing ratios using the
103 high frequency temperature and air pressure measurements. This is equivalent to the
104 traditional WPL correction [*e.g. Prytherch et al.*, 2010b]. Using *Bariteau et al.* [2010] we
105 calculate that our set-up gives a ~5 % error in the temperature dilution correction, which is

106 acceptable. The shrouded set-up is designed to reduce the sensor contamination from rain and
107 heavy sea spray, but the intake is not filtered. As a consequence a CO₂–H₂O cross-correlation,
108 which is most likely due to hygroscopic particles, was observed and additional correction for
109 this was made using the PKT method [Prytherch *et al.*, 2010a].

110 RESULTS AND DISCUSSION

111 The average EC F_{CO₂} calculated from the pre-PKT data is $-6.7 \times 10^{-2} \text{ mol m}^{-2} \text{ day}^{-1}$,
112 with a standard deviation of $0.27 \text{ mol m}^{-2} \text{ day}^{-1}$. The raw CO₂ flux has considerable scatter,
113 but there is a statistically significant ($\alpha < 0.05$) negative correlation with latent heat flux (F_{H₂O},
114 Fig. 2a) which shows that the data needs further correction. The average post-PKT F_{CO₂} is -
115 $0.61 \times 10^{-2} \text{ mol m}^{-2} \text{ day}^{-1}$, with a standard deviation of $0.11 \text{ mol m}^{-2} \text{ day}^{-1}$. This is comparable
116 to the CO₂ flux calculated using the Wanninkhof [1992] k-U_{10N} parameterization (-0.56×10^{-2}
117 $\text{mol m}^{-2} \text{ day}^{-1}$). The post-PKT F_{CO₂} still have considerable scatter, especially when the F_{H₂O} is
118 low, but there is no longer a negative correlation (Fig. 2b). It seems that when the F_{H₂O} is very
119 small the PKT method overcorrects and adds scatter to the data, leading to a relatively large
120 standard deviation in the corrected F_{CO₂}. The added scatter could be due to the dependence of
121 the PKT method on accuracy of F_{H₂O} measurements [Prytherch *et al.*, 2010a], and while
122 further tests using data with very low F_{H₂O} are necessary, it might be that the PKT method
123 needs to be modified to account for this. The post-PKT F_{CO₂} is small (Fig. 2b), but this is not
124 unexpected given the cold ocean and calm conditions (Fig. 3). The “flux” measured by the
125 null sensor is not significantly different from zero (Fig. 2c). The standard deviation in this
126 “flux” is an order of magnitude smaller than that of the post-PKT F_{CO₂}. Removing the null
127 “flux” removes scatter from the sample flux data, and the difference is statistically significant
128 with greater than 90 % confidence. This shows that even under very calm ocean conditions
129 having a null sensor to remove the bias from motion is valuable.

130 The undersaturation during the cruise was on average $-105 \pm 24 \mu\text{atm}$, whereas the end
131 of the cruise, where the water is also warmer and more saline, has lower $\Delta f\text{CO}_2$ (Fig. 3b). The
132 wind speed during the cruise ranged from 0.5 m s^{-1} to 10.8 m s^{-1} with a mean of $4.5 \pm 1.9 \text{ m s}^{-1}$
133 (Fig. 3c). The uncertainty is given as one standard deviation of the mean. 90 % of all wind
134 speed recorded were less than 7 m s^{-1} and 15 % less than 2.5 m s^{-1} so we have a quite large
135 data set of F_{CO_2} at very low wind speeds. No previously published EC experiment has
136 reported significant amounts of data at wind speeds less than 2.5 m s^{-1} so the Greenland Sea
137 experiment is in this respect unique.

138 Transfer velocity (k) was calculated from Eqn. 1 (reference) and bin averaged in 2 m s^{-1}
139 U_{10N} intervals (Fig. 4). The pre-PKT fluxes yield a very strong non-linear relationship in k -
140 U_{10N} , while the corrected fluxes have a k - U_{10N} relationship in the same range as the
141 *Wanninkhof* [1992] parameterization. The dramatic increase in the PKT correction with wind
142 speed was also seen in the flux data from the Southern Ocean Gas Exchange Experiment
143 [Edson *et al.*, 2011], and can be linked to the cubic relationship between CO_2 and H_2O mixing
144 ratios. We presume this is associated with the near-cubic wind-speed dependence of the
145 production of sea-salt aerosols [Lewis and Schwartz, 2004]. The variability is quite large,
146 however, and our data set is too small and the wind speed range too narrow to either confirm
147 previous or derive a new k - U_{10N} relationship.

148 CONCLUSIONS

149 Application of the PKT correction method to observations of EC CO_2 flux from the
150 Greenland Sea is successful in lowering the flux by an order of magnitude, thus making the
151 corrected fluxes comparable to established k - U_{10N} parameterizations. The data set is too small
152 to confirm previous studies and parameterizations. However, given the magnitude of the
153 correction needed for these data despite using shrouded, and thus somewhat weatherproofed,
154 sensors, it is clear that we need a more dedicated effort to understand the mechanisms causing

155 the large CO₂-H₂O crosstalk. Presented in this study are data at wind speeds less than 2.5 m s⁻¹,
156 ¹, and at the overall low wind speeds experienced during this cruise the flux of CO₂ is small
157 and the variability is large. This despite the large ΔfCO₂ which suggests that the potential for
158 carbon uptake is very large, but apparently not utilized in the summer due to low wind speeds.
159 It is thus unlikely to get a robust estimate of the size of the Greenland Sea carbon sink without
160 measurements in fall and winter.

161 ACKNOWLEDGEMENTS

162 This analysis has been funded by the Norwegian Research Council through the project
163 CARBON-HEAT (185093/S30). The 2006 Greenland Sea research cruise onboard R/V
164 G.O.Sars was funded by the CARBOOCEAN EU IP (5111176-2). This is publication XXXX
165 from the Bjerknes Centre for Climate Research.

166 REFERENCES

- 167 Bariteau, L., D. Helmig, C. W. Fairall, J. E. Hare, J. Hueber, and E. K. Lang (2010),
168 Determination of oceanic ozone deposition by ship-borne eddy covariance flux
169 measurements, *Atmos. Meas. Tech.*, *3*(2), 441-455.
- 170 Broecker, W. S., J. R. Ledwell, T. Takahashi, R. Weiss, L. Merlivat, L. Memery, T. H. Peng,
171 B. Jahne, and K. O. Munnich (1986), Isotopic versus micrometeorological ocean CO₂
172 fluxes - A serious conflict, *J. Geophys. Res.*, *91*(C9), 517-527.
- 173 Edson, J. B., A. A. Hinton, K. E. Prada, J. E. Hare, and C. W. Fairall (1998), Direct
174 covariance flux estimates from mobile platforms at sea, *J. Atmos. Oceanic Technol.*,
175 *15*(2), 547-562.
- 176 Edson, J. B., C. W. Fairall, L. Bariteau, C. J. Zappa, A. Cifuentes-Lorenzen, W. R. McGillis,
177 S. Pezoa, J. E. Hare, and D. Helmig (2011), Direct Covariance Measurement of CO₂
178 Gas Transfer Velocity during the 2008 Southern Ocean Gas Exchange Experiment:
179 Wind Speed Dependency, *submitted to J. Geophys. Res.*

181 Fairall, C. W., J. E. Hare, J. B. Edson, and W. R. McGillis (2000), Parameterization and
182 micrometeorological measurement of air-sea gas transfer, *Bound.-Layer Meteorol.*, *96*,
183 63-105.

184 Griessbaum, F., B. I. Moat, Y. Narita, M. J. Yelland, O. Klemm, and M. Uematsu (2010),
185 Uncertainties in wind speed dependent CO₂ transfer velocities due to airflow distortion
186 at anemometer sites on ships, *Atm. Chem. Phys.*, *10*(11), 5123-5133.

187 Ho, D. T., C. S. Law, M. J. Smith, P. Schlosser, M. Harvey, and P. Hill (2006), Measurements
188 of air-sea gas exchange at high wind speeds in the Southern Ocean: Implications for
189 global parameterizations, *Geophys. Res. Lett.*, *33*(16).

190 Hoover, T. E., and D. C. Berkshire (1969), Effects of hydration on carbon dioxide exchange
191 across an air-water interface, *J. Geophys. Res.*, *74*(2), 456.

192 Kolstad, E. W. (2008), A QuikSCAT climatology of ocean surface winds in the Nordic seas:
193 Identification of features and comparison with the NCEP/NCAR reanalysis, *J. Geophys.*
194 *Res.*, *113*(D11).

195 Kondo, F., and O. Tsukamoto (2007), Air-sea CO₂ flux by eddy covariance technique in the
196 equatorial Indian Ocean, *J. Oceanography*, *63*(3), 449-456.

197 Liss, P. S., and L. Merlivat (1986), Air-sea gas exchange rates: introduction and synthesis, in
198 *The Role of Air-Sea Exchange in Geochemical Cycling*, edited by P. Buat-Ménard, pp.
199 113-127, D. Reidel Publishing Company.

200 McGillis, W. R., J. B. Edson, J. E. Hare, and C. W. Fairall (2001a), Direct covariance air-sea
201 CO₂ fluxes, *J. Geophys. Res.*, *106*(C8), 16729-16745.

202 McGillis, W. R., J. B. Edson, J. D. Ware, J. W. H. Dacey, J. E. Hare, C. W. Fairall, and R.
203 Wanninkhof (2001b), Carbon dioxide flux techniques performed during GasEx-98, *Mar.*
204 *Chem.*, *75*, 267-280.

205 McGillis, W. R., et al. (2004), Air-sea CO₂ exchange in the equatorial Pacific, *J. Geophys.*
206 *Res.*, 109(C8).

207 Miller, S. D., T. S. Hristov, J. B. Edson, and C. A. Friehe (2008), Platform motion effects on
208 measurements of turbulence and air-sea exchange over the open ocean, *J. Atmos.*
209 *Oceanic Technol.*, 25(9), 1683-1694.

210 Miller, S. D., C. Marandino, and E. S. Saltzman (2010), Ship-based measurement of air-sea
211 CO₂ exchange by eddy covariance, *J. Geophys. Res.*, 115.

212 Moat, B. I., M. J. Yelland, R. W. Pascal, and A. F. Molland (2005), An overview of the
213 airflow distortion at anemometer sites on ships, edited, pp. 997-1006, John Wiley &
214 Sons Ltd.

215 Naegler, T., P. Ciais, K. Rodgers, and I. Levin (2006), Excess radiocarbon constraints on air-
216 sea gas exchange and the uptake of CO₂ by the oceans, *Geophys. Res. Lett.*, 33(11).

217 Nightingale, P. D., G. Malin, C. S. Law, A. J. Watson, P. S. Liss, M. I. Liddicoat, J. Boutin,
218 and R. C. Upstill-Goddard (2000), In situ evaluation of air-sea gas exchange
219 parameterizations using novel conservative and volatile tracers, *Global Biogeochem.*
220 *Cycles*, 14(1), 373-387.

221 Olsen, A., and A. Omar (2007), G.O.Sars Repeat Section 75N_2006 cruise data.
222 http://cdiac.ornl.gov/oceans/RepeatSections/clivar_75N.html, edited, Carbon Dioxide
223 Informatin Analysis Center, Oak Ridge National Laboratory, US Department of Energy,
224 Oak Ridge, Tennessee.

225 Pierrot, D., C. Neill, K. Sullivan, R. Castle, R. Wanninkhof, H. Luger, T. Johannessen, A.
226 Olsen, R. A. Feely, and C. E. Cosca (2009), Recommendations for autonomous
227 underway pCO₂ measuring systems and data-reduction routines, *Deep-Sea Res.*, 56(8-
228 10), 512-522.

229 Prytherch, J., M. J. Yelland, R. W. Pascal, B. I. Moat, I. Skjelvan, and C. C. Neill (2010a),
230 Direct measurements of the CO₂ flux over the ocean: Development of a novel method,
231 *Geophys. Res. Lett.*, 37(L03607).

232 Prytherch, J., M. J. Yelland, R. W. Pascal, B. I. Moat, I. Skjelvan, and M. A. Srokosz (2010b),
233 Open ocean gas transfer velocity derived from long-term direct measurements of the
234 CO₂ flux, *Geophys. Res. Lett.*, 37.

235 Sweeney, C., E. Gloor, A. R. Jacobson, R. M. Key, G. McKinley, J. L. Sarmiento, and R.
236 Wanninkhof (2007), Constraining global air-sea gas exchange for CO₂ with recent
237 bomb C-14 measurements, *Global Biogeochem. Cycles*, 21(2).

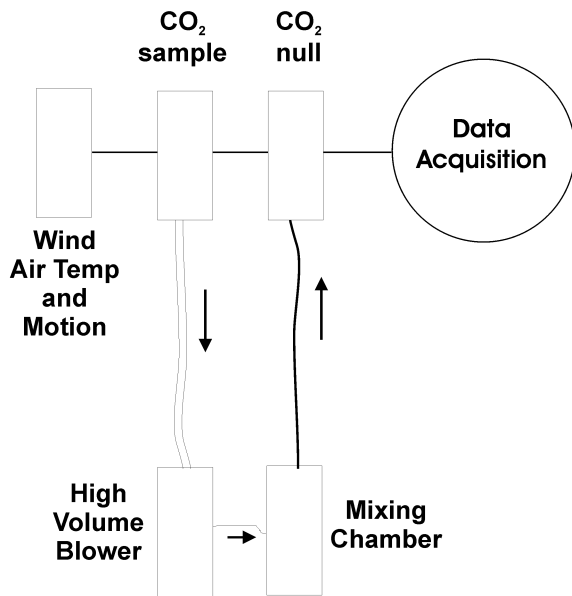
238 Wanninkhof, R. (1992), Relationship between wind speed and gas exchange over the ocean,
239 *J. Geophys. Res.* 97(C5), 7373-7382.

240 Wanninkhof, R., and M. Knox (1996), Chemical enhancement of CO₂ exchange in natural
241 waters, *Limnol. Oceanogr.*, 41(4), 689-697.

242 Wanninkhof, R., and W. R. McGillis (1999), A cubic relationship between air-sea CO₂
243 exchange and wind speed, *Geophys. Res. Lett.*, 26(13), 1889-1892.

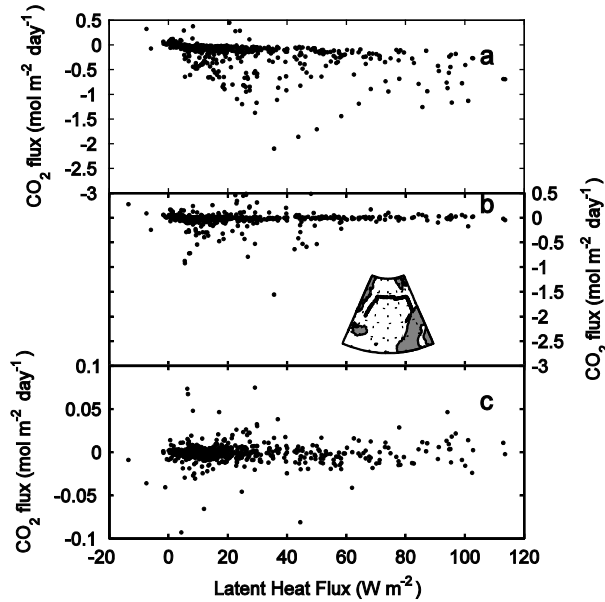
244 Webb, E. K., G. I. Pearman, and R. Leuning (1980), Correction of flux measurements for
245 density effects due to heat and water-vapor transfer, *Q. J. R. Meteorol. Soc.*, 106(447),
246 85-100.

247
248 FIGURES



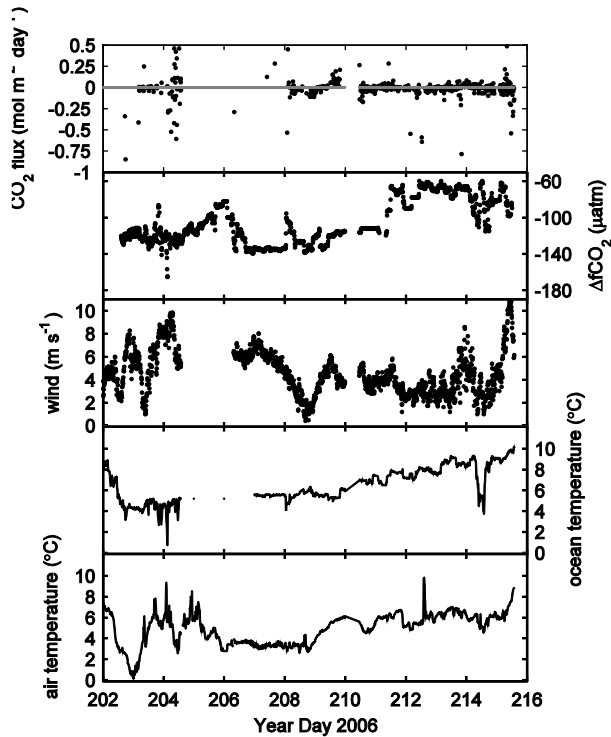
249
250

Figure 1. Schematic of the instrument set-up onboard R/V G.O.Sars July 21 – August 3, 2006.



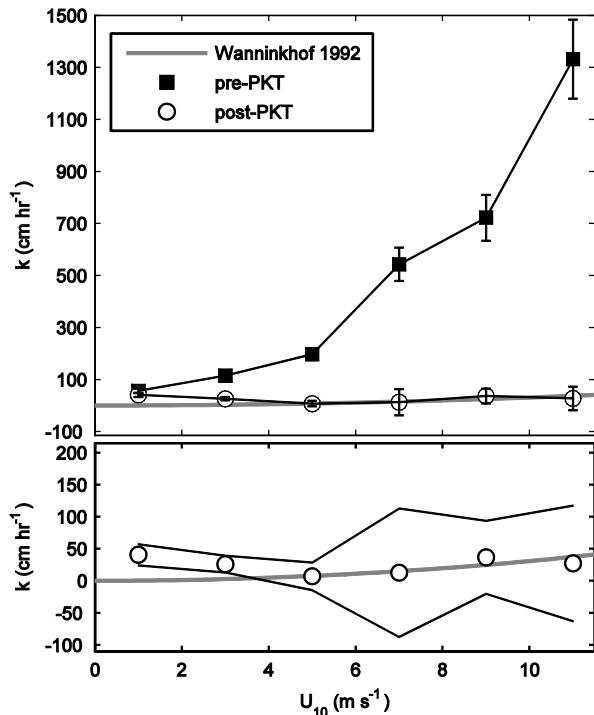
251
252
253
254
255
256

Figure 2. Eddy correlation CO₂ flux as a function of latent heat flux before and after the PKT correction. Two outliers are not shown on plot a (1.7 and $-6.3 mol m^{-2} day^{-1}$) and one on plot b ($-4.8 mol m^{-2} day^{-1}$). a) CO₂ flux from the sample LICOR before PKT correction, b) CO₂ flux from the sample LICOR after PKT correction, also shown is a map of the cruise track covered between July 21, 2006 and August 3, 2006 c) “flux” from the null LICOR. Note that this subplot has a different scale on the y-axis.



257
258
259

Figure 3. a) The temporal CO₂ flux with the zero line indicated in grey, b) the undersaturation ($\Delta f\text{CO}_2$), c) the sonic wind speed, d) the surface ocean temperature, and e) the air temperature during the cruise.



260
261
262
263
264
265

Figure 4. Top: The k bin-averaged in 2 m s^{-1} wind speed intervals plotted against U_{10N} . See the legend for details. The error bars show the standard error of the mean. Bottom: Close-up of the post-PKT k . The thin black lines show the 95 % confidence interval (estimated as plus or minus two times the standard error of the mean). The point at 11 m s^{-1} is based on only seven data points, and should not be given as much weight as the other points.